

Compton Scattering and Nucleon Polarisabilities in Chiral EFT: Status and Future

Harald W. Griebhammer,¹ Judith A. McGovern,² and Daniel R. Phillips³

¹*Institute for Nuclear Studies, Department of Physics,
George Washington University, Washington DC 20052, USA**

²*School of Physics and Astronomy, The University of Manchester, Manchester M13 9PL, UK*

³*Dept. of Physics and Astronomy, Institute of Nuclear and Particle Physics, Ohio University, Athens OH 45701, USA*

We review theoretical progress and prospects for determining the nucleon's static dipole polarisabilities from Compton scattering on few-nucleon targets, including new values and an emphasis on what polarised targets and beams can contribute; see Refs. [1–5] for details and a more thorough bibliography.

I. WHY COMPTON SCATTERING?

Let us start with an even simpler question: Why can you see any speaker at a conference? Light shines on matter, gets absorbed, and is re-emitted before it reaches your eyes. That is Compton scattering $\gamma X \rightarrow \gamma X$. A white shirt and red jumper reflect light differently because they have different chemical compositions: one re-emits radiation quite uniformly over the visible band, the other absorbs most non-red photons. The speaker's attire therefore not only shows their fashion sense (or lack thereof), but betrays information about the stuff of which they are made.

Let's be a bit more scientific. In Compton scattering $\gamma X \rightarrow \gamma X$, the electromagnetic field of a real photon induces radiation multipoles by displacing charged constituents and currents inside the target. The energy- and angle-dependence of the emitted radiation carries

information on the interactions of the constituents. In Hadronic Physics, it elucidates the distribution, symmetries and dynamics of the charges and currents which constitute the low-energy degrees of freedom inside the nucleon and nucleus, and – for nuclei – the interactions between nucleons, complementing information from one-photon data like form factors; see e.g. a recent review [1]. In contradistinction to many other electromagnetic processes, such structure effects have only recently been subjected to a multipole-analysis. The Fourier transforms of the corresponding temporal response functions are the proportionality constants between incident field and induced multipole. These *energy-dependent polarisabilities* parametrise the stiffness of the nucleon N (spin $\vec{\sigma}/2$) against transitions $Xl \rightarrow Yl'$ of given photon multipolarity at fixed frequency ω ($l' = l \pm \{0; 1\}$; $X, Y = E, M$; $T_{ij} = \frac{1}{2}(\partial_i T_j + \partial_j T_i)$; $T = E, B$). Up to about 400 MeV, the relevant terms are:

$$\begin{aligned} \mathcal{L}_{\text{pol}} = 2\pi N^\dagger [& \alpha_{E1}(\omega) \vec{E}^2 + \beta_{M1}(\omega) \vec{B}^2 + \gamma_{E1E1}(\omega) \vec{\sigma} \cdot (\vec{E} \times \dot{\vec{E}}) + \gamma_{M1M1}(\omega) \vec{\sigma} \cdot (\vec{B} \times \dot{\vec{B}}) \\ & - 2\gamma_{M1E2}(\omega) \sigma^i B^j E_{ij} + 2\gamma_{E1M2}(\omega) \sigma^i E^j B_{ij} + \dots \text{(photon multipoles beyond dipole)}] N \end{aligned} \quad (1)$$

The two spin-independent polarisabilities $\alpha_{E1}(\omega)$ and $\beta_{M1}(\omega)$ parametrise electric and magnetic dipole transitions. Of particular interest at present are now the four dipole spin-polarisabilities $\gamma_{E1E1}(\omega)$, $\gamma_{M1M1}(\omega)$, $\gamma_{E1M2}(\omega)$ and $\gamma_{M1E2}(\omega)$. They encode the response of the nucleon's spin structure, i.e. of the spin constituents, and complement JLab experiments at much higher energies. Intuitively interpreted, the electromagnetic field associated with the spin degrees causes birefringence in the nucleon (cf. classical Faraday-effect). Only the linear combinations γ_0 and γ_π of scattering under (0° and 180° scattering) are somewhat constrained by data or

phenomenology, with conflicting results for the proton (MAMI, LEGS) and large error-bars for the neutron.

The spin polarisabilities are of particular interest since they provide an excellent window into the photon-pion-nucleon system, i.e. into the charged pion cloud around the nucleon. While the $\gamma\pi$ interactions do not depend on the nucleon spin, the orientation of the pion cloud itself depends on the nucleon spin. Indeed, recall that the dominant πN and $\gamma\pi N$ interactions are related by minimal substitution, $\mathcal{L}_{\gamma\pi N} = -\frac{g_A}{2f_\pi} \vec{\sigma} \cdot (\vec{q} + e\vec{\epsilon})$, where \vec{q} is the pion momentum and $\vec{\epsilon}$ the photon polarisation. So both photon and pion emission or absorption is strongly dependent on the nucleon spin. As this picture persists at higher orders of the chiral expansion, Compton scattering with polarised photons on polarised nucleons provides stringent tests of χ EFT – and the spin polarisabilities are just the observables to look at.

* hgrie@gwu.edu; corresponding author. Invited Contribution to the 22ND INTERNATIONAL SPIN SYMPOSIUM (SPIN 2016), University of Illinois, Urbana (USA), 26-30 September 2016.

Since the polarisabilities are the parameters of a multipole decomposition, they do not contain more information than the full amplitudes, but characteristic signatures in specific channels are easier to interpret. For example, the strong ω -dependence of $\beta_{M1}(\omega)$ and $\gamma_{M1M1}(\omega)$ for $\omega \gtrsim 100$ MeV comes from the strong paramagnetic $\gamma N\Delta$ transition. The $\Delta(1232)$ thus enters dynamically well below the resonance region. The electric polarisability, in turn, exhibits a pronounced cusp at the pion-production threshold. As soon as an inelastic channel opens, namely at the pion-production threshold, the dynamical polarisabilities become complex, and their imaginary parts are directly related to the pion-photoproduction multipoles. Polarisabilities also test our understanding of the subtle interplay between electromagnetic and strong interactions: They enter in the two-photon-exchange contribution to the Lamb shift in muonic hydrogen [6]. And the Cottingham Sum rule relates the proton-neutron difference in β_{M1} to the proton-neutron electromagnetic mass difference. There is a cantankerous controversy about the precise nature of the relationship [7, 8], but there is little doubt that it tests our understanding of the subtle interplay between electromagnetic and strong interactions in a fundamental observable. Finally, nuclear targets provide an opportunity to study not only neutron polarisabilities, but indirectly also the nuclear force, since the photons couple to the charged pion-exchange currents.

II. WHERE WE ARE

The values $\alpha_{E1}(\omega = 0)$ etc. are often called “the (static) polarisabilities”; they compress the richness of information from data which is available in a wide range of energies between about 70 MeV and the Δ resonance region, extrapolating it into just a few numbers. In the canonical units of 10^{-4} fm^3 , the results of our most recent χ EFT extractions are, including an estimate of the residual theoretical uncertainties from order-by-order convergence (see Fig. 1 and [2, 4]):

$$\begin{aligned} \alpha_{E1}^{(p)} &= 10.65 \pm 0.35_{\text{stat}} \pm 0.2_{\text{Baldin}} \pm 0.3_{\text{th}} \\ \beta_{M1}^{(p)} &= 3.15 \mp 0.35_{\text{stat}} \pm 0.2_{\text{Baldin}} \mp 0.3_{\text{th}} \\ \alpha_{E1}^{(n)} &= 11.55 \pm 1.25_{\text{stat}} \pm 0.2_{\text{Baldin}} \pm 0.8_{\text{th}} \\ \beta_{M1}^{(n)} &= 3.65 \mp 1.25_{\text{stat}} \pm 0.2_{\text{Baldin}} \mp 0.8_{\text{th}} \end{aligned} \quad (2)$$

For the proton, we checked statistical data consistency, made sure the results are compatible with the Baldin Sum rule, fit polarisabilities at $\omega \lesssim 170$ MeV and $\Delta(1232)$ parameters above that, iterated until convergence is reached, and finally find a satisfactory $\chi^2 = 113.2$ for 135 degrees of freedom. The fit quality for the neutron is addressed below.

We also predicted the spin values [2, 5], prior to the first MAMI data taken at 290 MeV, which provide the first significant constraints on individual proton spin polarizabilities [9] (in their canonical units of 10^{-4} fm^4):

$$\begin{array}{rcc} & \gamma_{E1E1} & \gamma_{M1M1} \\ \chi\text{EFT neutron} & -4.0 \pm 1.9_{\text{th}} & 1.3 \pm 0.5_{\text{stat}} \pm 0.6_{\text{th}} \\ \chi\text{EFT proton} & -1.1 \pm 1.9_{\text{th}} & 2.2 \pm 0.5_{\text{stat}} \pm 0.6_{\text{th}} \\ \text{proton MAMI} & -3.5 \pm 1.2 & 3.2 \pm 0.9 \end{array} \quad \begin{array}{rcc} & \gamma_{E1M2} & \gamma_{M1E2} \\ & -0.1 \pm 0.6_{\text{th}} & 2.4 \pm 0.5_{\text{th}} \\ & -0.4 \pm 0.6_{\text{th}} & 1.9 \pm 0.5_{\text{th}} \\ & -0.7 \pm 1.2 & 2.0 \pm 0.3 \end{array} \quad (3)$$

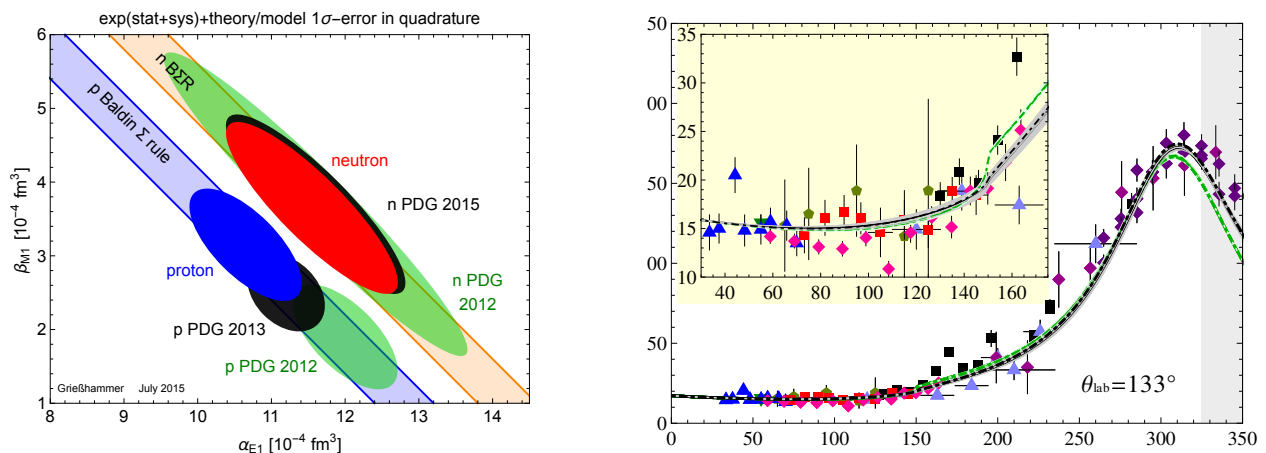


FIG. 1. *Top*: Static scalar polarisabilities in our fits (red: proton; blue: neutron); PDG listings prior to (green) and after our extractions (black). 1σ errors, with statistic, systematic and theory error added in quadrature. *Bottom*: Example of data and χ EFT result, with fit uncertainties, as function of ω ; see Ref. [2] for details.

A major concerted experimental effort at HI γ S, MAMI

and MAXlab will provide new, high-accuracy data – in

cluding on observables with beam and/or target polarisations; see e.g. [10, 11]. Interpretation of such data of course requires commensurate theory support. One must carefully evaluate the consistency of the data to reveal hidden systematic errors; subtract binding effects in few-nucleon systems; extract the polarisabilities; identify their underlying mechanisms and relate them to QCD – and all that with reproducible theoretical uncertainties and minimal theoretical bias.

Prompted by experimental colleagues, theorists with backgrounds in several variants of Dispersion Relations and Effective Field Theories summarised the present common theoretical understanding as follows [12]. (1) Static polarisabilities can be extracted from future data well below the pion-production threshold with high theoretical accuracy and minimal theory error. (2) Data around and above the pion production threshold show increased sensitivity to the spin polarisabilities and will help to understand and resolve some discrepancies between different approaches. (3) All theoretical approaches resort to well-motivated but not fully controlled approximations around and above the $\Delta(1232)$ resonance. In the longer term, theorists welcome a complete set of experiments up to the pion production threshold to disentangle detailed information from the energy dependence of the Compton multipoles.

III. CHIRAL EFFECTIVE FIELD THEORY

χ EFT, the low-energy theory of QCD and extension of Chiral Perturbation Theory to few-nucleon systems, has been quite successful in proton and few-nucleon Compton scattering. Its purely-mesonic sector is Chiral Perturbation Theory (χ PT); and its one-nucleon sector is Baryon χ PT, or Heavy-Baryon χ PT, when an additional expansion in the nucleon mass as a heavy scale is employed which reduces the theory to a non-relativistic one at leading-order. χ EFT generates the most general amplitude consistent with gauge invariance, the pattern of chiral-symmetry breaking, and Lorentz covariance. With explicit $\Delta(1232)$ degrees of freedom, its low-energy scales are the pion mass $m_\pi \approx 140$ MeV; the Delta-nucleon mass splitting $\Delta_M \approx 290$ MeV; and the photon energy ω . When measured in units of a natural “high” scale $\Lambda \approx 800$ MeV at which this variant can be expected to break down because new degrees of freedom become dynamical, Pascalutsa and Phillips identified one common parameter with magnitude smaller than 1: $\delta \equiv \frac{\Delta_M}{\Lambda} \approx \left(\frac{m_\pi}{\Lambda}\right)^{1/2}$, where the latter is a convenient numerical coincidence [13]. Recently, we derived single-nucleon Compton amplitudes from zero energy up to about 350 MeV. For $\omega \lesssim m_\pi$, they contain all contributions at $\mathcal{O}(e^2\delta^4)$ (N⁴LO, accuracy $\delta^5 \lesssim 2\%$), and for $\omega \sim \Delta_M$ all at $\mathcal{O}(e^2\delta^0)$ (NLO, accuracy $\delta^2 \lesssim 20\%$) [1, 2].

A reproducible, rigorous and systematically improvable *a priori* estimate of theoretical accuracies of observables, as in Eqs. (2) and (3) or Fig. 7, is of course essential

to uniquely disentangle chiral dynamics from data. Since the χ EFT result is ordered in powers of $\delta < 1$, it provides just that. Recently, the procedure to justify such estimates was codified into a Bayesian statistical interpretation of the truncation errors underlying standard EFT estimates [14]. We applied this to construct the probability distributions of the theoretical uncertainties quoted in Eqs. (2) and (3); see Ref. [5] and references therein. Since it does not employ comparison with experiments but is based on information which is intrinsic to the EFT expansion, the results fulfil a fundamental criterion of the scientific method: falsifiability.

Such an uncertainty assessment is of course also vital for reliable extractions of *neutron* polarisabilities since one must model-independently subtract nuclear binding effects from few-nucleon data. Figure 2 shows examples of the three classes of contributions in few-nucleon systems. Charged exchange currents and rescattering often dominate over the targeted nucleonic structure contributions. An analysis of Compton scattering therefore also provides indirect, non-trivial benchmarks as to how accurately the chiral expansion accounts order-by-order for nuclear binding and its mesonic contributions. For the deuteron, our results are complete at $\mathcal{O}(e^2\delta^3)$ or N³LO from the Thomson limit up to about 120 MeV, including the $\Delta(1232)$ degree of freedom [1].

Recently, 22 points were added to the deuteron database by MAXlab [4, 15]. This first new data in over a decade effectively doubled the deuteron’s world dataset. Our analysis shows that it is fully consistent with and within the world dataset ($\chi^2 = 45.2$ for 44 degrees of freedom), and with the Baldin sum rule. Using the same Bayesian methods as in our determinations of the proton and spin polarisabilities in Eqs. (2) and (3), we assessed the theoretical uncertainty as ± 0.8 . These data alone slashed the statistical error by 30%, with new values adopted by the 2015 PDG. Just to illustrate the data quality, the χ^2 distribution of the new world dataset agrees with the analytic expectation; see Fig. 3.

IV. WHERE WE WANT TO BE

The future lies in unpolarised, single-polarised and double-polarised experiments of high accuracy, and in theoretical analyses with reproducible systematic uncertainties. To understand the subtle differences of the pion clouds around the proton and neutron induced by explicit chiral symmetry breaking in QCD, we need to know the neutron polarisabilities with uncertainties comparable to those of the proton – Eq. (2) shows that this is mostly an issue of better data (and some theory work which is under way). Therefore, MAMI, MAXlab and HI γ S aim for deuteron data with statistical and systematic uncertainties of better than 5%, and plan extensions to ³He and ⁴He. In general, heavier nuclei are experimentally better to handle and provide count rates which scale at least linearly with the target charge when photons scat-

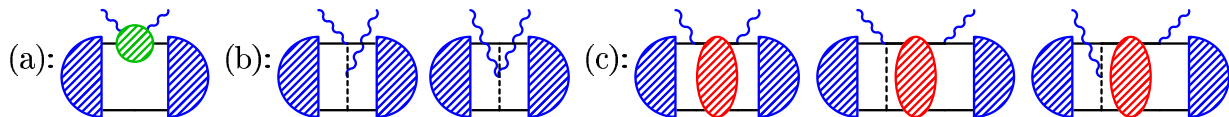


FIG. 2. Contributions to deuteron Compton scattering. Ellipse: NN S -matrix: (a): single-nucleon; (b) photon coupling to charged exchange currents which bind the nucleus as dictated by chiral symmetry; (c) rescattering between emission and absorption restores the low-energy Thomson limit and guarantees current conservation.

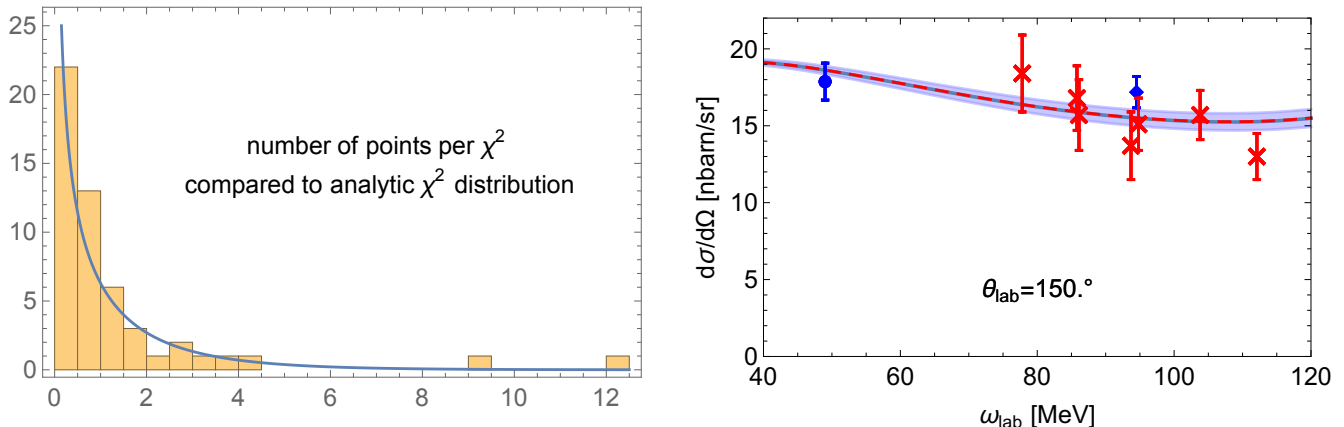


FIG. 3. *Top*: Histogram of the number of deuteron Compton data with a given χ^2 , overlaid with the predictions of an ideal, statistically consistent set with 1 degree of freedom (1 datum singled out, all others fixed). The two data with $\chi^2 \geq 9$ are pruned by statistical-likelihood criteria; including them does not have a significant impact on the neutron values. We add point-to-point and angle-dependent systematic errors in quadrature to the statistical error, and subsume overall systematic errors into a floating normalisation. The norm of each dataset floats by $\leq 5\%$ and within the respective quoted normalisation errors of the data. *Bottom*: Example of data and χ EFT result, with fit uncertainties (red: new MAXlab data); see Refs. [4, 15] for details.

ter incoherently from the protons, i.e. for $\omega \gtrsim 100$ MeV. But a theoretical description of their energy levels with adequate accuracy is involved. For the proton, amplitudes on the $\lesssim 2\%$ -level for $\omega \lesssim m_\pi$ and $\lesssim 20\%$ around the Δ resonance are available; for deuteron and ${}^3\text{He}$, we now extend descriptions with similar accuracies into the Delta resonance region. Around ${}^3\text{He}$ - ${}^4\text{He}$ - ${}^6\text{Li}$ may well be the “sweet-spot” between the needs and desires of theorists and experimentalists. For example, we updated the single-nucleon parts of the ${}^3\text{He}$ code to the same order $e^2\delta^3$ as in the deuteron. Figure 4 shows that excluding the energy-dependence due to the $\Delta(1232)$ can lead to false signals in high-accuracy extractions of neutron polarisabilities. As in the deuteron, the effect is increased at back-angles, but forward-rates are suppressed; see Ref. [16] for details.

Since the four spin-polarisabilities for each nucleon – which, as yet, are hardly explored – probe the spin-constituents of the nucleon, they are a top priority of experiment and theory alike. Sensitivity studies have been performed in χ EFT variants with and without explicit $\Delta(1232)$; see Fig. 5 and summary in [1, Sec. 6.1]. The MAMI experiment and extraction for the proton agrees well with our χ EFT findings, although both extraction and χ EFT are at too high an energy to be really reliable, see Eq. (3) and Fig. 5.

Recently, the deuteron cross section and asymmetry with arbitrary photon and target polarisations have also been parametrised via 18 independent observables [3]. Particularly interesting are some asymmetries which turn out to be sensitive to only one or two polarisabilities. For spin polarisabilities with an error of $\pm 2 \times 10^{-4} \text{ fm}^4$, asymmetries should be measured with an accuracy of 10^{-2} or so, with differential cross sections of a dozen nb/sr at 100 MeV or a few dozen nb/sr at 250 MeV. Relative to single-nucleon Compton scattering, interference with the deuteron’s D wave and pion-exchange current increases the sensitivity to the “mixed” spin polarisabilities γ_{E1M2} and γ_{M1E2} . A *Mathematica* file for $\omega < 120$ MeV is available from hgr1e@gwu.edu (see screen-shot in Fig. 6), and more are being finalised for the proton and ${}^3\text{He}$.

It is well-recognised that polarised ${}^3\text{He}$ is (approximately) a polarised neutron target. Corrections to this statement can be quantified using ab initio wave functions calculated with χ EFT potentials. χ EFT suggests the photon beam asymmetry with a transversely polarised target, Σ_{2x} , is the cleanest observable in which to determine neutron spin polarisabilities. It is affected by $\gamma_{M1M1}^{(n)}$ much more strongly than it is by the scalar polarisabilities – and unaffected by any proton spin polarisabilities. Other neutron spin polarisabilities affect this observable, but manifest a different angular dependence.

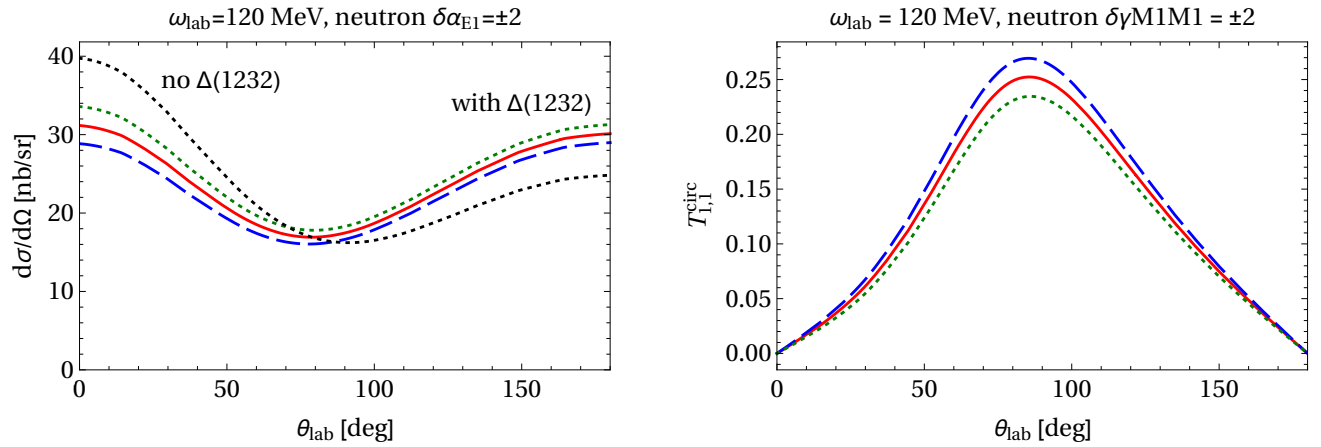


FIG. 4. ${}^3\text{He}$ Compton scattering at 120 MeV. *Top*: with $\Delta(1232)$ (red solid), and without (black dotted); blue dashed/green dotted: $\alpha_{E1}^{(n)} \pm 2$ [16]. *Bottom*: Sensitivity of the asymmetry $T_{11}^{\text{circ}} = -\sqrt{2}\Sigma_{2x}$ with $\Delta(1232)$ on $\gamma_{M1M1}^{(n)}$ [16].

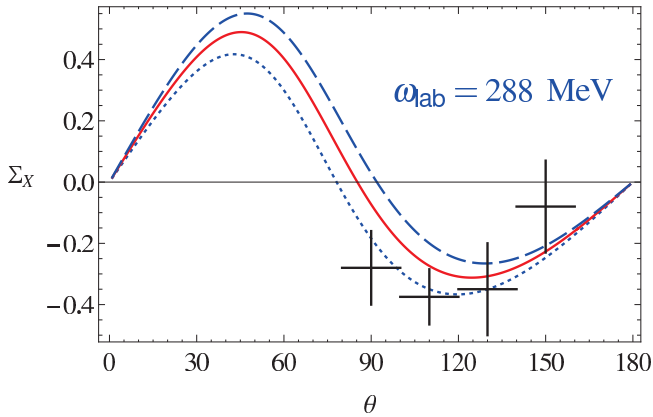


FIG. 5. χEFT prediction and MAMI data [9] for the double-polarisation observable Σ_{2x} on the proton. Solid: $\gamma_{E1E1} = -1.1$ (predicted); dashed/dotted: uncertainties of spin polarisabilities from Eq. (3) and Ref. [5] (other χEFT truncation errors not included).

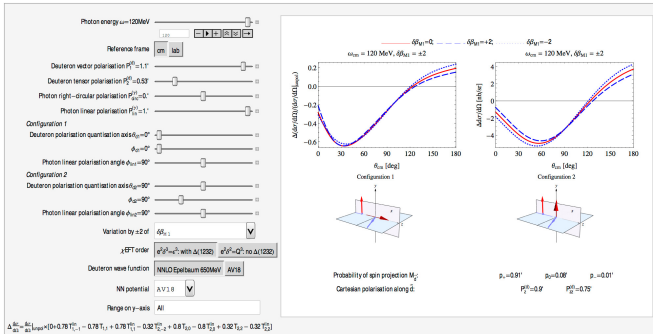


FIG. 6. *Mathematica* screenshot for deuteron Compton scattering with arbitrary polarisations [3].

In fact, as ${}^3\text{He}$ is doubly charged and contains more nucleon pairs, interference of polarisability effects with

proton Thomson terms and meson-exchange currents is larger than for the deuteron or proton. It may therefore be that neutron spin polarisabilities can ultimately be determined more accurately than proton ones—if the necessary target densities can be reached; see Fig. 4.

Finally, χEFT connects data with emerging lattice-QCD computations by reliable extrapolations from numerically less costly, heavier pion masses within the χEFT regime to the physical point and circumvents a direct lattice computation of Compton scattering – that would be highly nontrivial. Lattice computations, in turn, test to what extent χEFT adequately captures the m_π -dependence of the low-energy dynamics, and may predict short-distance (fit) parameters from QCD, as an alternative to determining them experimentally. A particularly interesting χEFT prediction is a rather strong isovector component away from the physical point for both α_{E1} and β_{M1} , arising from an intricate interplay of the chiral physics of the pion cloud and short-distance effects. The NPLQCD collaboration published intriguing lattice results for the proton’s and neutron’s β_{M1} at $m_\pi = 806$ MeV [17]; see Fig. 7 and Ref. [5]. The *difference* $\beta_{M1}^{(p)} - \beta_{M1}^{(n)}$ is nearly identical to the chiral result even well beyond the range in which χEFT should be applicable. This suggests that the experimental finding $\beta_{M1}^{(p)} \approx \beta_{M1}^{(n)}$ is something of a coincidence. The agreement with lattice computations for α_{E1} is even better [5].

ACKNOWLEDGMENTS

HWG cordially thanks the organisers, in particular for their scheduling flexibility; and the audience for the strong reaction to a last-minute idea how to start the talk. This work was supported in part by UK Science and Technology Facilities Council grants ST/J000159/1 and ST/L005794/1 (JMcG), by the US Department of Energy under contracts DE-FG02-93ER-40756 (DRP) and DE-

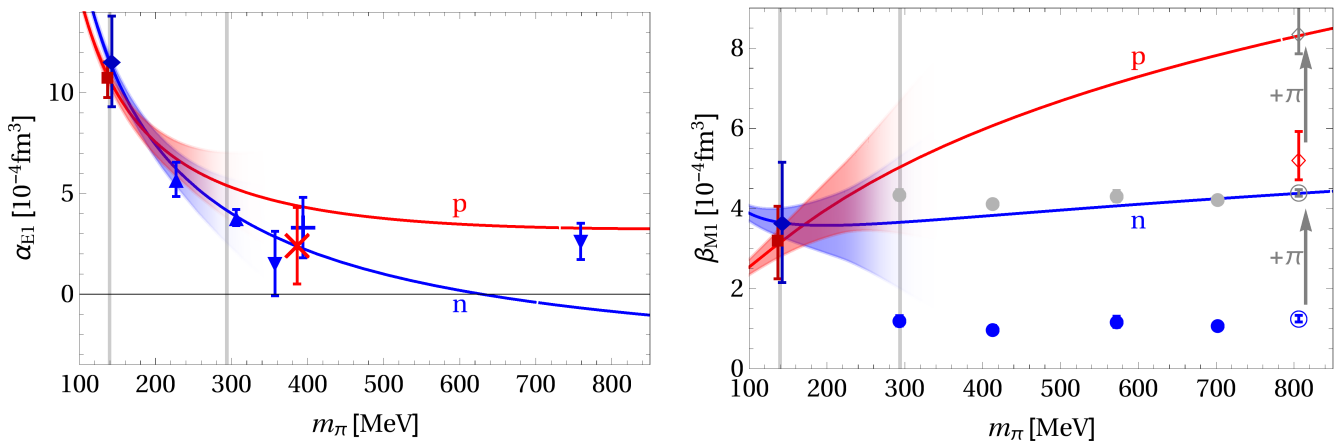


FIG. 7. Comparison of our χ EFT *predictions* to lattice computations [5]. Red/blue lines with red/blue error corridors: our χ EFT results. Corridors represent theoretical uncertainties in the regime where χ EFT can be expected to converge and fade out as the uncertainty estimate becomes less reliable. Error-bars at the physical point add statistical, theory and Baldin-sum-rule errors linearly, as applicable. *Left:* α_{E1} : \blacktriangle (neutron) Lujan et al. [18]; \times (proton) and $+$ (neutron) Detmold et al. [19]; \blacktriangledown (neutron) Engelhardt/LHPC [20, 21]. *Right:* β_{M1} : \bullet (neutron) Hall et al. [22]; \diamond (proton) and \circ (neutron) NPLQCD [17]. Gray “ghost points” found by shifting all lattice results by $+\pi \times 10^{-4} \text{ fm}^3$ [*sic!*].

FG02-95ER-40907 (HWG), and by the Dean’s Research

Chair programme of the Columbian College of Arts and Sciences of The George Washington University (HWG).

-
- [1] H. W. Griebhammer, J. A. McGovern, D. R. Phillips and G. Feldman, *Prog. Part. Nucl. Phys.* **67** (2012) 841 [arXiv:1203.6834].
- [2] J.A. McGovern, D.R. Phillips, H.W. Griebhammer, *Eur. Phys. J. A* **49** (2013) 12 [arXiv:1210.4104 [nucl-th]].
- [3] H. W. Griebhammer, *Eur. Phys. J. A* **49** (2013) 100 [arXiv:1304.6594 [nucl-th]].
- [4] L. S. Myers, J. Annand, J. Brudvik, G. Feldman, K. Fissum, H. Griebhammer, K. Hansen and S. Henshaw [COMPTON@MAX-lab Collaboration], *Phys. Rev. Lett.* **113** (2014) 262506 [arXiv:1409.3705 [nucl-ex]].
- [5] H. W. Griebhammer, J. A. McGovern and D. R. Phillips, *Eur. Phys. J. A* **52** (2016) 139 [arXiv:1511.01952 [nucl-th]].
- [6] R. Pohl, R. Gilman, G. A. Miller and K. Pachucki, *Ann. Rev. Nucl. Part. Sci.* **63** (2013) 175 [arXiv:1301.0905 [physics.atom-ph]].
- [7] A. Walker-Loud, C.E. Carlson, G.A. Miller, *Phys. Rev. Lett.* **108** (2012) 232301 [arXiv:1203.0254 [nucl-th]].
- [8] J. Gasser, M. Hoferichter, H. Leutwyler and A. Rusetsky, *Eur. Phys. J. C* **75** (2015) no. 8, 375 [arXiv:1506.06747 [hep-ph]].
- [9] P. P. Martel *et al.* [A2 Collaboration], *Phys. Rev. Lett.* **114** (2015) 112501 [arXiv:1408.1576 [nucl-ex]].
- [10] H. R. Weller, *Prog. Part. Nucl. Phys.* **62** (2009) 257.
- [11] G. M. Huber and C. Collicott, arXiv:1508.07919 [nucl-ex].
- [12] H. W. Griebhammer, A. I. L’vov, J. A. McGovern, V. Pascalutsa, B. Pasquini and D. R. Phillips, arXiv:1409.1512 [nucl-th].
- [13] V. Pascalutsa and D. R. Phillips, *Phys. Rev. C* **67** (2003) 055202 [nucl-th/0212024].
- [14] R. J. Furnstahl, N. Klco, D. R. Phillips and S. Wesolowski, *Phys. Rev. C* **92** (2015) no. 2, 024005 [arXiv:1506.01343 [nucl-th]].
- [15] L. Myers, J. Annand, J. Brudvik, G. Feldman, K. Fissum, H. Griebhammer, K. Hansen and S. Henshaw [COMPTON@MAX-lab Collaboration], *Phys. Rev. C* **92** (2015) 025203 [arXiv:1503.08094 [nucl-ex]].
- [16] B. Strandberg, A. Margaryan, H. W. Griebhammer, J. A. McGovern, D. R. Phillips and D. Shukla, forthcoming.
- [17] E. Chang, W. Detmold, K. Orginos, A. Parreno, M. J. Savage, B. C. Tiburzi and S. R. Beane [NPLQCD Collaboration], *Phys. Rev. D* **92** (2015) no. 11, 114502 [arXiv:1506.05518 [hep-lat]].
- [18] M. Lujan, A. Alexandru, W. Freeman, F. Lee, *PoS LATTICE* **2014** (2014) 153 [arXiv:1411.0047 [hep-lat]].
- [19] W. Detmold, B. C. Tiburzi and A. Walker-Loud, *Phys. Rev. D* **81** (2010) 054502 [arXiv:1001.1131 [hep-lat]].
- [20] M. Engelhardt [LHPC Collaboration], *Phys. Rev. D* **76** (2007) 114502 [arXiv:0706.3919 [hep-lat]].
- [21] M. Engelhardt, *PoS LAT* **2009** (2009) 128 [arXiv:1001.5044 [hep-lat]].
- [22] J. M. M. Hall, D. B. Leinweber, R. D. Young, *Phys. Rev. D* **89** (2014) 054511 [arXiv:1312.5781 [hep-lat]].